Sequence-specific inhibition of Dicer measured with a force-based microarray for RNA ligands

Katja Limmer, Daniela Aschenbrenner and Hermann E. Gaub*

Lehrstuhl für Angewandte Physik and Center for Nanoscience (CeNS), Ludwig-Maximilians-Universität, Amalienstrasse 54, 80799 Munich, Germany

ABSTRACT

Malfunction of protein translation causes many severe diseases, and suitable correction strategies may become the basis of effective therapies. One major regulatory element of protein translation is the nuclease Dicer that cuts double-stranded RNA independently of the sequence into pieces of 19–22 base pairs starting the RNA interference pathway and activating miRNAs. Inhibiting Dicer is not desirable owing to its multifunctional influence on the cell's gene regulation. Blocking specific RNA sequences by small-molecule binding, however, is a promising approach to affect the cell's condition in a controlled manner. A label-free assay for the screening of site-specific interference of small molecules with Dicer activity is thus needed. We used the Molecular Force Assay (MFA), recently developed in our lab, to measure the activity of Dicer. As a model system, we used an RNA sequence that forms an aptamer-binding site for paromomycin, a 615-dalton aminoglycoside. We show that Dicer activity is modulated as a function of concentration and incubation time: the addition of paromomycin leads to a decrease of Dicer activity according to the amount of ligand. The measured dissociation constant of paromomycin to its aptamer was found to agree well with literature values. The parallel format of the MFA allows a large-scale search and analysis for ligands for any RNA sequence.

INTRODUCTION

The enzyme Dicer has increasingly been attracting attention owing to its crucial role in the RNA interference (RNAi) pathway. RNAi is an endogenous means used by cells to regulate protein translation at the post-transcriptional level (1). Single-stranded RNA sequences of 18–25 nucleotides bind to specific mRNAs and hinder protein translation. Although various classes of small regulatory RNA have been identified, two main categories of single-stranded RNA (ssRNA) involved in metazoan RNA interference can be distinguished that differ in their origin and function but share processing by Dicer: short-interfering RNA (siRNA) and microRNA (miRNA). siRNA precursors are long fully complementary dsRNA that are typically introduced directly into the cytoplasm or taken up from the environment, though recent findings suggest that siRNA may also originate from endogenous sources like transposons (2). Hence, the main task of the siRNA-processing machinery seems to be the defense of genome integrity in response to foreign or invasive nucleic acids (3). miRNAs are transcribed and pre-processed in the nucleus into incomplete base-paired stem-loop structures, known as pre-microRNAs. They are then transferred to the cytoplasm, where Dicer matures the pre-miRNA by cleaving the stem loop structure. The mature miRNA strand binds to the mRNA and usually inhibits translation in combination with a protein complex known as RNA-induced silencing complex (RISC) (4), although gene up-regulation by the RISC complex has also been reported (5,6). In contrast to siRNA, which requires total complementarity to its target sequence, miRNAs and their target mRNA do not need to base-pair perfectly so that a certain miRNA can bind and regulate a variety of mRNA sequences. Several miRNAs may also play a role in the regulation of a single mRNA transcript. Thus, miRNA seems to fine-tune protein expression. The amount of the various miRNA strands differs according to cell age, cell type and health status (7). So miR-1 appears to be tissue specific and was only found in heart tissue and somites of mice embryos (8). Evidence is accumulating that miRNAs are critical for many cellular processes such as developmental timing, cell proliferation or stem cell division (9). Consequently, many disease states occur or are sustained by miRNA dysregulation (10). miR-21, for example, was up-regulated in all tumour samples analysed by (11). Therefore, targeting the RNAi pathway at the step of Dicer cleavage is a promising approach for new therapies against illnesses like cancer or metabolic diseases.

*To whom correspondence should be addressed. Tel: +49 89 2180 3172; Fax: +49 89 2180 2050; Email: gaub@physik.uni-muenchen.de

A relatively small protein of <250 kDA, Dicer has been found in the cytoplasm of all eukaryotes studied to date (12), sometimes in several variants with different tasks. For instance in Drosophila, Dicer-1 cuts pre-miRNA while Dicer-2 generates siRNA from long dsRNA precursors (13). The L-shape of the protein seems to be well-conserved for all variants. Recognition of dsRNA by a PAZ domain occurs in the head of Dicer, which is separated from the two RNAse III domains by a ruler domain (Figure 2A). The base of the L is formed by a helicase, whose function is not totally understood (12). Dicer cleaves long and short (>30 nt) dsRNA strands with equal efficiency, whereas duplexes of ≤21 nt are not processed *in vitro*. A 3′ 2-nucleotide-long overhang, a characteristic of pre-microRNA molecules, increases Dicer's efficiency compared with blunt ends (14).

To interfere with RNAi, knocking out Dicer is not advisable owing to Dicer's crucial role for several cellular processes. On the other hand, a small molecule that binds to the pre-miRNA in question with high specificity and hinders Dicer from maturing the miRNA in question is a great drug candidate. The difficulty, herein, lies in finding potential ligands that bind a certain RNA sequence with high selectivity and also interfere with Dicer cleavage. Krützfeldt *et al.* (15) demonstrated that single-stranded cholesterol-conjugated 2′-O-methyl oligoribonucleotides, complementary to a certain miRNA and termed antagomirs, could specifically reduce the level of that miRNA *in vivo*. Elmen *et al.* (16) could reversibly decrease the level of plasma cholesterol by silencing miRNA-122 with a modified antagomir in non-human primates, thus exemplifying the possible therapeutic value of antagomirs. In both studies, already mature miRNAs are silenced, which might impair the potency of these molecules, as mature miRNA are included in the protein complex RISC and are probably less accessible than pre-miRNA. Cellular uptake of oligonucleotides is another difficulty so that Krützfeldt *et al.* needed high doses to see an effect. Thus, targeting pre-miRNA structures with small molecules has several advantages, but the research of small-molecule RNA binding has encountered several problems [for a review see (17)]. Especially an easy high-throughput technique to screen for and characterize RNA binders could speed up the progress of finding suitable molecules.

Our technique of the Molecular Force Assay (MFA) provides a fast and reliable tool to screen for different RNA binders, to characterize them and to quantify their ability to prevent Dicer from cutting. The MFA is a highly parallel technique, described in detail in (18) and (19), to measure unbinding forces comparatively so that small changes in the structural stability of molecular complexes can be detected. Two molecular bonds, a sample and a reference bond, are linked in series between two surfaces. One surface is retracted and a force gradually builds up in the molecular complexes until one of the bonds breaks. A fluorophor attached to the linking sequence between the two molecular complexes stays with the intact bond (Figure 1A) so that a simple fluorescent measurement by means of a commercially available epi-fluorescent microscope may detect the outcome. Thus,

the mechanical stability of two molecular interactions can be probed and compared with each other. In contrast to other force-probe techniques like atomic force microscopy (AFM) or optical traps that measure the unbinding force by a spring-like macroscopic object like a cantilever, the MFA reduces the force detector to the microscopic scale of another molecule, a known reference DNA duplex, so that small differences in structural stability like the binding of a ligand may be resolved. The setup of the MFA is designed such that a large number of molecular complexes are tested simultaneously in one experiment on one chip, and the outcome of this experiment gives statistically significant information on the nature of the molecular interaction in question. Furthermore, as the MFA measures the interaction force between the molecules, unspecific binding events or complex backgrounds like serum do not alter the experimental outcome. Thus, the MFA allows us to detect and characterize the binding of a small molecule to a number of different oligonucleotides or of many small molecules to a certain RNA or DNA sequence in a format, where the analytes are not altered, e.g. by labelling. So far, the MFA has been applied to detect single-nucleotide polymorphism (20), study differences in antibody/antigen interactions (21), investigate the chiral selectivity of small peptides (22), characterize the binding properties of an aptamer to its ligand in a molecularly crowded ambient (23) and to analyse protein–DNA interaction (19).

Here, a 35 bp RNA duplex functions as a substrate for Dicer and is tested against a 22 bp or 27 bp DNA double strand that does not interact with Dicer. The two molecular complexes are linked in a zipper configuration so that a force stretching the bonds unzips the two duplexes (Figure 1A). The construct is covalently attached to the glass slide at the bottom and via a biotin–streptavidin–biotin complex to the upper poly(dimethylsiloxane) (PDMS) stamp surface (Figure 1A). The cyanine dye Cy5 between the RNA and DNA duplex stays with the intact bond after the rupture process, while a second fluorophor Cy3, conjugated to the 3′ end of the uppermost strand, constitutes a Fluorescence Resonance Energy Transfer (FRET) pair with the Cy5 and quantifies the constructs that have not properly coupled to the upper surface and, thus, have not been under force load. If Dicer cuts off about 20 bp of the RNA duplex, this bond is weakened and breaks with higher probability. Thus, Dicer activity can be detected and is quantified for different amounts of Dicer and incubation times. As a proof of principle, the RNA double strand incorporates an RNA aptamer specific for the aminoglycoside paromomycin, which we will characterize by measuring the dissociation constant. It is to be expected that the interaction of paromomycin with its aptamer will hinder Dicer from binding to the RNA duplex and, thus, from cutting.

MATERIALS AND METHODS

DNA/RNA constructs

The molecular complexes consist of three strands that are successively hybridized in our laboratory and are shown in
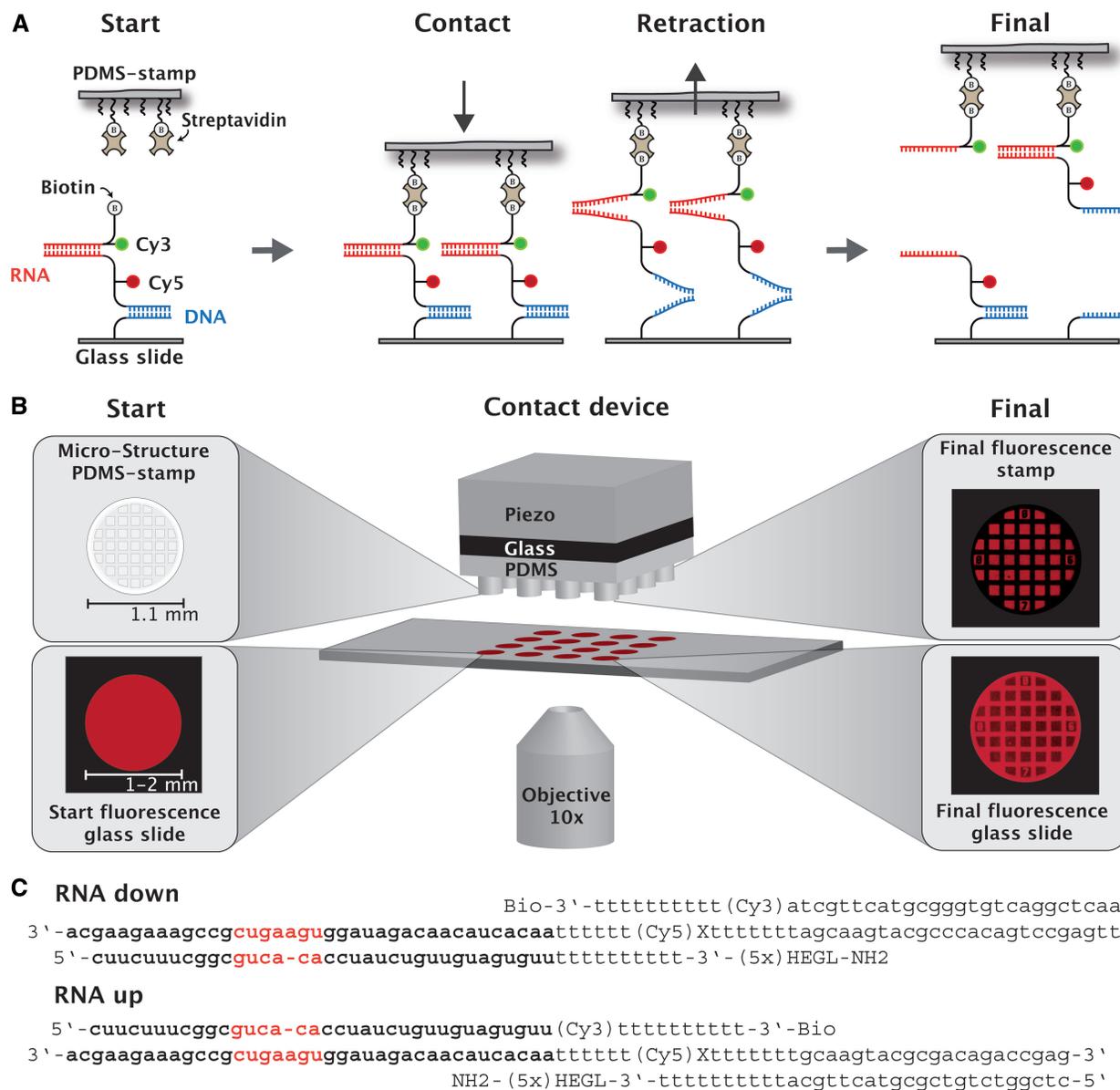
Figure 1. Schematics of the Molecular Force Assay. (**A**) The molecular complex is built up by covalently attaching the lowest strand to a glass slide and, subsequently, binding the pre-hybridized upper duplex to the lowest strand. The fluorophor Cy5 is conjugated to a poly-T sequence connecting the two duplexes. The upper strand is labelled with Cy3 so that a FRET signal provides a measure for a correctly hybridized molecular construct. The 'RNA up' geometry is defined with the DNA complex attached to the glass slide and the RNA duplex constituting the upper part. A biotin–streptavidin–biotin bond links the molecular complex to the upper surface, a soft PDMS stamp. Upon retracting the PDMS stamp, a force builds up in the molecular constructs and unzips the duplexes until the weaker of the two bonds in series ruptures. Note that in this format Cy5 serves as marker for those molecular complexes which remain intact. (**B**) In the setup, the contact device is mounted on an inverted microscope. The PDMS stamp features a micropattern that facilitates leveling and drainage of liquid during the contact and separation process. The oligonucleotide constructs are spotted in a 4×4 pattern, and fluorescence intensities are measured before and after the contact and separation process. After separation the fluorescence intensities of the molecules remaining on the glass and the PDMS surface add up to the total fluorescence intensity measured at the beginning. (**C**) Nucleic acid sequences of the molecular constructs in both configurations.

Figure 1C. The lowermost is modified with an amino group in order to covalenty attach the oligonucleotides to a surface. Avoiding surface effects, 5 HEGL (hexaethyleneglycol) molecules act as an additional spacer between the amino group and the oligonucleotides. Furthermore, poly-T separate the double-stranded sequences from the surfaces and each other. The cyanine dyes Cy5 and Cy3 are attached by a *N*-hydroxysuccinimide ester to the middle and uppermost strand, respectively, at a distance of six nucleobases in the hybridized complex to act as a FRET pair. The medium strand is inverted in the middle by inverse amidites since the force to melt a DNA or RNA double strand depends on the direction of the helix to which the force is applied. The RNA complex features a two nucleotide overhang at the 3′ end in order to maximize Dicer processing (14). Proving the validity of our results, we carried out all experiments in parallel with both possible geometries.

If the RNA target duplex is attached to the glass slide and the DNA complex constitutes the upper part, we call this configuration 'RNA down'. The other geometry with the RNA complex the upper part and the DNA duplex bound to the glass slide we named 'RNA up' (Figure 1C). We bought all oligonucleotides with the modifications from IBA GmbH, Germany.

Slide preparation

All aqueous solutions necessary for the chemical procedures described here were treated with 0.1% Diethyl pyrocarbonate (DEPC) over night and were autoclaved afterwards in order to avoid RNAse contamination. We pipetted 1 µl of the lowermost strand in a concentration of 25 µM in 5× SSC buffer (saline sodium citrate; Sigma-Aldrich GmbH, Germany) on an aldehydesilane-coated glass slide (Nexterion Slide AL, Pequlab, Germany) in a 4 × 4 pattern and incubated it over night in a humid atmosphere. The slide was rinsed thoroughly with ddH_2O and incubated in a 1% aqueous solution of $NaBH_4$ (VWR Scientific GmbH, Germany) for 90 min in order to reduce the Schiff bases and render the linkage of the oligonucleotide to the slide covalent. Unreacted groups were blocked in 1× SSC containing 4% bovine serum albumin (Sigma-Aldrich GmbH; Germany), minimizing unspecific binding. We placed a custom-made 16-well silicone isolator (Grace-Biolabs; USA) on top of the immobilized lowermost oligomer and transferred to each well 3 µl of 0.2 µM of the upper complex in 5× SSC, which had been heated and cooled down over several hours in a thermocycler beforehand to avoid undesired secondary structures. After an hour hybridization, the molecular complexes as diplayed in Figure 1A were completed. Unbound strands were removed by several washing steps with different salt concentrations (2× SSC, 0.2× SSC, 1× SSC). Care was taken that the samples were kept in an aqueous environment at all times.

Incubation of ligands

For all measurements detecting Dicer activity, the glass slide with the molecular bonds was fastened to a custom-made PMMA well with a silicone lip seal. According to the desired incubation time and quantity, the recombinant human Dicer protein in a concentration of 1 U/µl (Life technologies, UK) was directly pipetted into the PMMA well prior to the contact process. We applied amounts between 0.5 and 5 µl Dicer solution. For measurements with paromomycin and Dicer, the appropriate amount of paromomycin (paromomycin sulphate salt, Sigma, Germany) was directly mixed with the solution of 1× SSC of the last washing step and, thus, added before Dicer. The paromomycin titration experiments were executed on one glass slide within the spotted 4 × 4 pattern of oligonucleotides. The custom-made 16-well silicone isolator (Grace-Biolabs; USA) allows the incubation of every spot with a different solution by means of a self-made microfluidic system driven by two 16-channel peristaltic pumps (Ismatec GmBH; Germany). Hence, a whole titration curve can be recorded within a single experiment.

Stamp preparation

Micro- and macrostructured PDMS stamps were fabricated by casting 1:10 crosslinker/base (Sylgard, Dow Corning, MI, USA) into a custom-made Pyrex/silicon wafer (HSG-IMIT, Germany) according to standard procedures (24). The resulting PDMS stamps feature pillars of 1 mm diameter and height with a spacing of 3 mm in a square pattern on a 3-mm-thick basis and are cut in pieces of 4 × 4 pillars. The flat surface of the pillars is microstructured with 100 × 100 µm pads separated by 41 µm wide and 5 µm deep rectangular trenches enabling the drainage of liquid during the contact and separation process (Figure 1B). For the surface functionalization, the cleaned stamp surface was first activated in 12.5% HCl overnight and derivatized with (3-glycidoxypropyl)-trimethoxysilane (ABCR, Germany) in order to generate epoxide groups. 1:1 methoxy-PEG-NH$_2$ (MW 2000 Dalton) and Biotin-PEG-NH$_2$ (MW 3400 Dalton) (Rapp-Polymere, Germany) were melted at 80°C, and ~1 µl was transferred to each pillar followed by overnight incubation at 80°C in an Argon atmosphere. The excess polymers were thoroughly removed by rinsing with ddH_2O. Shortly before the experiment, the stamps were incubated in 0.4% BSA in 1× SSC containing 1 µg/µl Streptavidin (Thermo Fisher Scientific, Germany) for 30 min, washed with 0.05% Tween 20 (VWR Scientific GmbH, Germany) in 0.2× SSC and gently dried with N_2 gas.

Contact process and fluorescence read-out

The functionalized stamp adheres upside-down to the glass block glued to a closed-loop piezoelectric actuator (PZ 400, Piezo Systems Jena, Germany) and a DC motorized translation stage (Physik Instrumente GmbH, Germany), as shown in Figure 1B. The slide with the oligonucleotide constructs is fixed beneath the stamp on a stainless steel stage with permanent magnets so that every stamp pillar meets a 1–2 mm diameter spot of oligonuclotides on the glass slide. The whole contact device is mounted on an inverted microscope (Axio Observer Z1, Carl Zeiss MicroImaging GmbH, Germany) with an xy-DC motorized high-accuracy translation stage (Physik Instrumente GmbH, Germany). Contact is made by means of the piezo, and care is taken that each individual pillar is not compressed more than 3 µm. The planar adjustment of stamp and slide as well as the contact process are controlled by reflection interference contrast microscopy (25). To let the biotin of the oligonucleotides bind to the streptavidin coating of the PDMS stamp, the contact between stamp and slide is maintained for 10 min. The piezo retracts the stamp with a velocity of 1 µm/s in all experiments, and a force builds up in the double strands until the weaker one breaks with higher probability. Quantifying the number of intact bonds in relation to total molecular constructs, fluorescence images of the Cy5 intensity are taken before and after the contact process. As it cannot be assumed that all oligonucleotides have bound to the stamp, their contribution has to be substracted. Therefore, a fluorescence picture of the FRET intensity between the Cy3 of

the upper strand and the Cy5 label of the middle strand, being a measure of the integrity of the upper molecular complex, is taken before and after the contact process as well. Three outcomes are possible: First, the lower bond broke so that no fluorescence, neither Cy5 nor FRET signal, can be detected. Second, the upper bond broke so that the Cy5 intensity can be measured but no FRET signal. Third, the molecular construct did not bind to the stamp, which means that the Cy5 and FRET intensity are unchanged except for bleaching. The quotient of the image taken after the contact process to the image taken before, $F_{Cy5} = I_{Cy5}^{Final}/I_{Cy5}^{Start}$ and $F_{FRET} = I_{FRET}^{Final}/I_{FRET}^{Start}$, cancels out inhomogeneities due to the Gaussian illumination profile and surface defects, rendering the MFA rather robust. The normalized fluorescence is given by $NF = \frac{F_{Cy5} - F_{FRET}}{1 - F_{FRET}}$. A detailed description can be found in (26). The normalized fluorescence is thus the fraction of intact lower bonds of the total number of molecules under load.

RESULTS AND DISCUSSION

Characterization of Dicer activity

Initially, we developed a platform for analysing the protein Dicer. The schematic outline and RNA sequences are shown in Figure 1. We built a molecular complex comprising a 35 bp double-stranded RNA duplex covalently bound to a glass slide at one end, and covalently attached to a 27 bp reference DNA duplex at the other end. Dicer could be titrated in solution to the completed molecular constructs, and the surfaces were separated after incubation times varying between 60 and 300 min. Figure 2B depicts the results of such a measurement upon addition of 1 µl of Dicer to every sample except the first, which acts as a reference value. The normalized fluorescence at time t = 0 provided a value of $NF = 0.79 \pm 0.01$. An initial value at time t = 0 of $NF = 0.5$, corresponding to two complexes nearly identical in their structural stability, would be desirable to resolve small differences in stability induced through binding of a ligand or mismatch. However, our system was designed to quantify enzymatic RNAse activity. Because Dicer cuts off around 20 bp, we designed our sytem such that the RNA complex before Dicer cleavage was stronger than the DNA, while the RNA complex after Dicer cleavage was weaker than the reference DNA duplex. As in our system the RNA construct is 8 bp longer than the DNA complex, in the absence of Dicer, the weaker DNA reference bond ruptures with higher probability. In the 'RNA down' configuration, the RNA complex is attached directly to the glass slide; therefore, the likelihood for the Cy5 label to be found at the lower surface is higher than at the upper surface, and the normalized fluorescence lies around $NF = 0.8$. If Dicer cleaves off about 20 bp of the RNA double strand, the lower molecular complex is weakened and the normalized fluorescence decreases (Figure 2B). Dicer processes the RNA duplex in multiple enzymatic turnovers. Consequently the normalized fluorescence declined further with increasing incubation time (Figure 2B). Our experimental design provides Dicer with an excess of

substrate, dsRNA, so that the substrate concentration can be assumed constant and the reaction rate of Dicer is solely limited by the amount of Dicer present. Thus, a linear relation of the normalized fluorescence to Dicer processing time was expected and verified by our measurement. The slope of the fit was used as a measure of the rate of Dicer processing, allowing us to quantify Dicer activity.

Proof of Principle of the microarray test format for RNA ligands

Next, we analysed the binding properties of the aminoglycoside of the neomycin family, paromomycin, to its RNA aptamer by means of the MFA. The structure of this aptamer and its ligand-binding behaviour are well-known and described in detail in (28) and (29). The aptamer sequence was incorporated into our RNA duplex 11 nucleotides from the 3' end, and was located within the portion of the RNA duplex cleaved by Dicer. We hypothesized that this position could disrupt Dicer interaction with the RNA duplex. Every second spot in the 16-spot pattern of oligonucleotide constructs bound to the glass slide were incubated for at least 1 h with a different concentration of paromomycin in 1× SSC, ranging from 0 to 1995 µM, so that a single experiment resulted in a full titration curve with two values for every concentration paromomycin. The experiment was carried out several times for both the 'RNA up' and 'RNA down' configurations. From the resulting values for the normalized fluorescence, the mean and standard error of the mean were calculated so that every data point represents between two and four experiments. The data were fitted by a hill equation isotherm that accounts for specific and non-specific binding by means of the software package GraphPad Prism 5 (GraphPad Software, San Diego, CA, USA). The result for the 'RNA up' configuration is shown in Figure 2D, which yielded a dissociation constant of 2.55 ± 2.18 µM and negligible unspecific binding. Literature reports values of 0.2–1 µM depending on the technique (29,30), in agreement with our results. The measurements in the 'RNA down' geometry resulted in dissociation constants of about 100 ± 70 µM (data not shown), which deviated by a factor 50 from our other measurements with the inverted geometry. Non-specific binding of the ligand to the surfaces or molecular complexes would be identical in both configurations, so we attributed the increase in dissociation constant for the 'RNA down' configuration to the proximity of the RNA construct to the glass slide. Notwithstanding the passivation of the glass slide, the RNA duplex in the 'RNA down' configuration presumably stretches across the surface, which might reduce the accessibility of the RNA aptamer binding pocket for the ligand paromomycin, resulting in an apparent increase in the dissociation constant. Consequently, the 'RNA down' configuration with the ligand-binding part integrated in the lower complex does not seem suited for the characterization of a RNA-binding ligand. In contrast, providing the ligand-binding sequence with a spacer and locating away from the surface by implementing it in the upper RNA duplex yielded reliable values for the dissociation constant
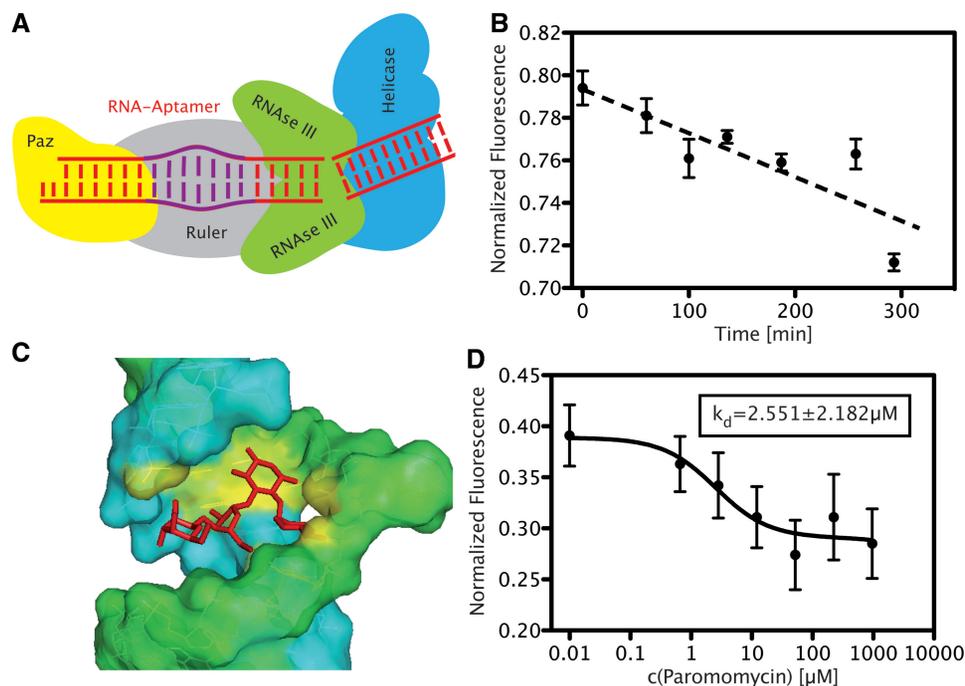
Figure 2. Characterization of molecules in question. (**A**) Schematics of Dicer and its sub-domains. (**B**) The activity of Dicer is measured in an excess of substrate so that the processing rate is constant. Accordingly, the normalized fluorescence decreases linearly with incubation time. The data were measured in the 'RNA down' configuration. (**C**) Schematic picture of paromomycin (red) binding to its RNA aptamer. The two strands of the RNA duplex are displayed in blue and green, while the bases interacting with the ligand are coloured in yellow [PDB: 1J7T by (27)]. (**D**) Titration of the ligand paromomycin to the complexes in the 'RNA up' geometry increasingly stabilizes the upper RNA duplex so that the normalized fluorescence decreases. The fluorescence data were fitted by a Hill equation isotherm.

in agreement with literature values. Although the dissociation constants measured by other more laborious and time-consuming techniques might be more accurate, our assay provides sufficiant accuracy in a parallel screening format for dissociation constants, ranging from the picomolar (26) (chiral polyamides binding to DNA) to the high micromolar scale (23) (DNA-aptamer specific for ATP). Moreover, the current format with 16 spots can be varied to titrate two ligands in parallel (eight spots per ligand) or change the binding sequence in half the spots in order to gain a deeper insight into the ligand-binding sequence interaction in a one-shot experiment.

Hinderance of Dicer processing by ligand binding

In the next step, we prepared four different slides with our oligonulceotide constructs in the 'RNA down' configuration as well as in the 'RNA up' configuration. The initial value for NF was determined in pure buffer (Figure 3A). To the second sample, we added 2.5 μl of the Dicer solution and separated the surfaces after 60 min, while we incubated the third sample with 1 mM paromomycin at least 1 h before the measurement (Figure 3B and C). The buffer of the fourth sample contained 1 mM paromomycin, and 2.5 μl Dicer solution was added 60 min before separation of the surfaces (Figure 3D). The first sample acted as reference and gave $NF = 0.34 \pm 0.01$ (standard deviation) in the 'RNA up' configuration. The addition of Dicer weakened the

upper RNA double strand by cutting off around 20 basepairs so that the flurophor was found more often on the lower side. Therefore, the NF increased to 0.40 ± 0.02, as displayed in Figure 3E. Upon binding of paromomycin, the RNA duplex was stabilized and the NF decreased to 0.27 ± 0.01 in the third case. If paromomycin hinders Dicer from cutting the RNA duplex, we expect that the fourth measurement yields NF close to the ligand-only case, but at least below the $NF = 0.40$ obtained for measurement with only Dicer in the solution. As shown in Figure 3E, we measured an NF of 0.30 ± 0.01, which is close to the result of only paromomycin. From these data, we concluded that Dicer was definitely hindered by binding of paromomycin, but not completely blocked. The 'RNA down' configuration yielded the same outcome (Figure 3F).

Correction of fluorescence data

During the measurments with the 'RNA down' configuration, we found that the quantum yield of the fluorophors, especially of the Cy5, varied slightly owing to the changing local environment. In particular, the fluorescence intensity of Cy5 increased if the upper strand ruptured leaving behind the single-stranded overhang. This leads to the phenomenon that the normalized fluorescence value can adopt values above one in the 'RNA down' configuration (see raw data in the Supplementary Data). Levitus and co-workers reported a change of fluorescence intensity upon interaction of Cy3 with single and double-stranded
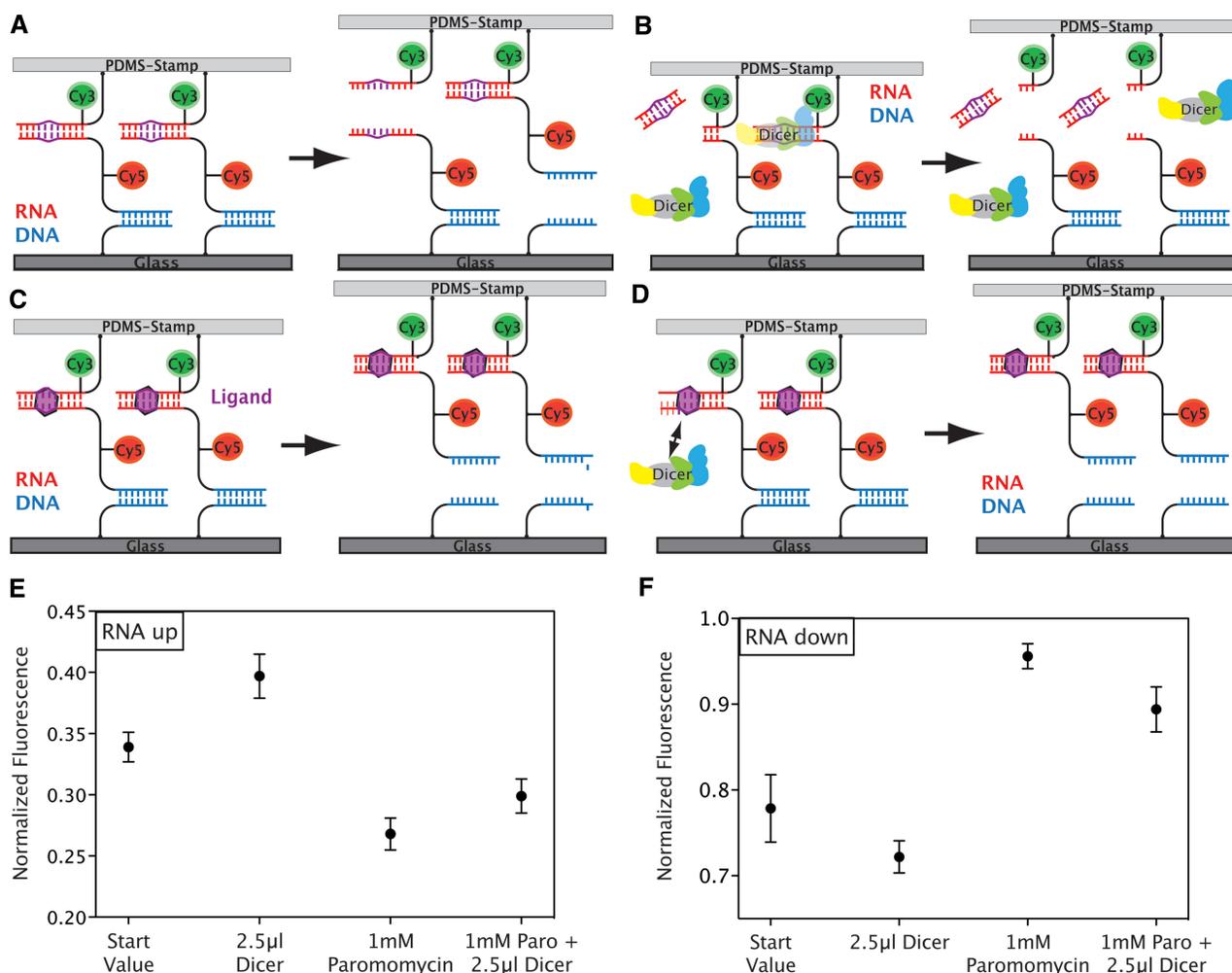
Figure 3. Dicer inhibition. (**A**) Separating the molecular constructs in the absence of Dicer or ligand provides an initial value in the 'RNA up' geometry for the *NF* of 0.34 ± 0.01. (**B**) Upon addition of Dicer, the protein cleaves off around 20 bp of the RNA duplexes and weakens the upper part so that the balance of the fluorophor distribution is shifted towards the lower side and the *NF* increases to 0.40 ± 0.02. (**C**) Binding of the ligand to its aptamer strengthens the RNA complex and the fluorophor distribution after rupture of the molecular complexes is shifted towards the upper surface, decreasing the *NF* to 0.27 ± 0.01. (**D**) Upon addition of Dicer and ligand, binding of the ligand to the RNA duplex blocks Dicer and strengthens the upper complex so that the *NF* yields 0.30 ± 0.01, which is close to the value we measured with ligand only. (**E**) Display of the data measured in the experiment just described. (**F**) Inverting the geometry yields the same result in reverse. From an initial value of 0.78 ± 0.02, the *NF* decreases to 0.72 ± 0.01 through the destabilization by Dicer. Ligand binding strengthens the lower RNA duplex and shifts the *NF* to higher values of 0.96 ± 0.01. If Dicer is hindered from cutting by ligand binding, the *NF* with 0.90 ± 0.01 stays close to the value measured with ligand only.

DNA. They attributed this change to the blocking of non-radiative decay pathways of the excited state fluorophor by steric hindrance (31). In (32), a similar behaviour for Cy5 is described. Although the Cy5 label is, in our case, always conjugated to the middle single strand and six basepairs away from both duplexes, an interaction between the fluorophor and the oligonucleotide duplex seems a plausible explanation for the observed increase in fluorescence intensity. Because the Cy3 is only measured as part of a duplex, any effect due to interactions with the oligonucleotides cancels out in the ratio. To correct the Cy5 fluorescence intensities, we measured the intensity of its emisson spectrum in bulk solution in both cases, the single middle strand and the complete upper duplex, by fluorescence spectroscopy and calculated a quenching factor F (see Supplementary Data).

Determining the experimental error for F, we calculated the maximum range of possible factors and re-analysed our data measured by the MFA. Although all measured data points are shifted to smaller *NF* values, the outcome of the experiments and the corresponding conclusions remain unchanged (see Supplementary Figure S1). For further analysis, we therefore chose a medium value for the quenching factor of $F = 1.19$ for the 'RNA down' geometry, and $F = 1.06$ for the 'RNA up' geometry and corrected all measured data accordingly.

Minimum amount of ligand necessary for Dicer inhibition

We investigated what concentration of paromomycin is nessecary to hinder Dicer from cleaving. We incubated samples in the 'RNA down' configuration with

paromomycin, with the concentration ranging from 0.66 to 224 μM, and added 2.5 μl Dicer solution 1 h before the separation. The result is displayed in Figure 4. The lowest concentration of 0.66 μM paromomycin did not affect Dicer processing, but already a concentration of 2.82 μM partially inhibited Dicer, whereas 52 μM paromomycin hindered most of Dicer processing.The dissociation constant, which we had determined in the previous section to be 2.55 ± 2.18 μM, agrees nicely with the finding here, that a paromomycin concentration in this range leads to a partial inhibition of the cleavage process. It points directly towards a close relationship between the dissociation constant of a ligand and its potential to hinder Dicer processing. For ligands that bind thighter to their RNA sequence, we expect a blocking of Dicer at lower concentrations of the ligand.

CONCLUSION

In a proof of principle, we demonstrated that the function of the protein Dicer can be selectively blocked by a ligand that sequence specifically binds to the RNA. Our MFA reliably detected processing of the RNA duplex as well as the binding of a small ligand to RNA, which resulted in an inhibition of Dicer. In contrast to other techniques (33), the MFA requires neither labelling of the target sequence, nor the ligand or protein. It only needs flurophors well-separated from the area of interest so that the interaction of the molecules in question is not disrupted and can be analysed undisturbed. The localization of our molecular constructs between two surfaces is both an advantage and a drawback at the same time. Because we measure interaction forces rather than the mere presence of a ligand, our assay can easily test different ligand–oligonucleotide interactions in parallel without interfering background signals from the bulk or the need for stringent washing procedures. But possible surface effects e.g. non-specific adhesion between ligand or oligonucleotides
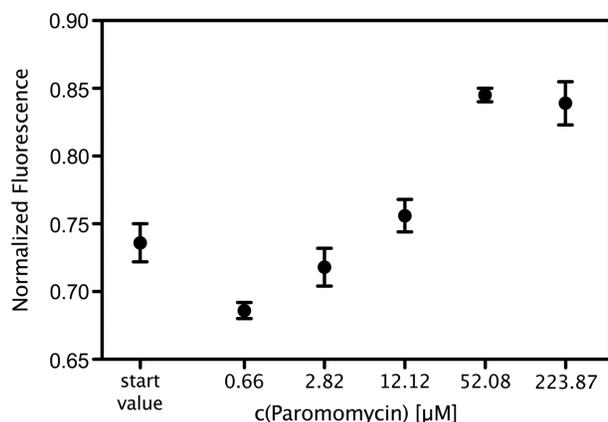
and surface have to be carefully excluded. Furthermore, our assay allows us to analyse the interaction of Dicer with our RNA construct and the interaction of the ligand to its binding sequence separately without changing the molecular complexes. This ensures that Dicer cleavage is blocked by hindering the protein to bind to its substrate not by any interaction between Dicer and the ligand. In addition, we illustrated the capability of our assay to characterize RNA-binding molecules in a one-shot experiment, enabling examination of the binding behaviour of a large number of molecules with moderate effort. The current setup allows to test 16 different systems in parallel, either one substance against 16 different DNA or RNA sequences or one oligonucleotide construct against 16 different ligands or concentrations of one ligand or a combination of both. To expand the multiplexing capabilities of our setup towards high throughput, the amount of reacting agent has to be reduced to a minimum and the number of RNA sequences have to be increased. Microfluidic devices can drastically diminish the reaction volume, and DNA/RNA spotting techniques allowed us to test eight different systems within $100 \times 100 \, \mu m^2$ (19,34). With further standardization and development, our technique of the MFA has the potential to become the first force-based high throughput technique.

Figure 4. Paromomycin efficiency. To determine the minimum amount of paromomycin necessary to block Dicer, we prepared samples in the 'RNA down' configuration with different amounts of paromomycin and added 2.5 μl Dicer solution 1 h before the measurement. We found that 0.66 μM paromomycin has no effect, but already 2.82 μM paromomycin hinders Dicer processing, while for 52.08 μM paromomycin, all Dicer activity is blocked.

REFERENCES

1. Mello,C.C. and Conte,D. Jr (2004) Revealing the world of RNA interference. *Nature*, **431**, 338–342.
2. Siomi,H. and Siomi,M.C. (2009) On the road to reading the RNA-interference code. *Nature*, **457**, 396–404.
3. Carthew,R.W. and Sontheimer,E.J. (2009) Origins and Mechanisms of miRNAs and siRNAs. *Cell*, **136**, 642–655.
4. Bartel,D.P. (2004) MicroRNAs: genomics, biogenesis, mechanism and function. *Cell*, **116**, 281–297.
5. Vasudevan,S., Tong,Y. and Steitz,J.A. (2007) Switching from repression to activation: microRNAs can up-regulate translation. *Science*, **318**, 1931–1934.

6. Orom,U.A., Nielsen,F.C. and Lund,A.H. (2008) MicroRNA-10a binds the 5'UTR of ribosomal protein mRNAs and enhances their translation. *Mol. Cell*, **30**, 460–471.

7. Ambros,V. (2011) MicroRNAs and developmental timing. *Curr. Opin. Genet. Dev.*, **21**, 511–517.

8. van Rooij,E. (2011) The art of microRNA research. *Cir. Res.*, **108**, 219–234.

9. Shruti,K., Shrey,K. and Vibha,R. (2011) Micro RNAs: tiny sequences with enormous potential. *Biochem. Biophys. Res. Commun.*, **407**, 445–449.

10. Friedman,J.M. and Jones,P.A. (2009) MicroRNAs: critical mediators of differentiation, development and disease. *Swiss Med. Wkly.*, **139**, 466–472.

11. Conti,A., Aguennouz,M., La Torre,D., Tomasello,C., Cardali,S., Angileri,F.F., Maio,F., Cama,A., Germano,A., Vita,G. *et al.* (2009) miR-21 and 221 upregulation and miR-181b downregulation in human grade II-IV astrocytic tumors. *J. Neurooncol.*, **93**, 325–332.

12. Lau,P.W., Guiley,K.Z., De,N., Potter,C.S., Carragher,B. and MacRae,I.J. (2012) The molecular architecture of human Dicer. *Nat. Struct. Mol. Biol.*, **19**, 436–440.

13. Lee,Y.S., Nakahara,K., Pham,J.W., Kim,K., He,Z., Sontheimer,E.J. and Carthew,R.W. (2004) Distinct roles for Drosophila Dicer-1 and Dicer-2 in the siRNA/miRNA silencing pathways. *Cell*, **117**, 69–81.

14. Vermeulen,A., Behlen,L., Reynolds,A., Wolfson,A., Marshall,W.S., Karpilow,J. and Khvorova,A. (2005) The contributions of dsRNA structure to Dicer specificity and efficiency. *RNA*, **11**, 674–682.

15. Krützfeldt,J., Rajewsky,N., Braich,R., Rajeev,K.G., Tuschl,T., Manoharan,M. and Stoffel,M. (2005) Silencing of microRNAs *in vivo* with 'antagomirs'. *Nature*, **438**, 685–689.

16. Elmen,J., Lindow,M., Schutz,S., Lawrence,M., Petri,A., Obad,S., Lindholm,M., Hedtjarn,M., Hansen,H.F., Berger,U. *et al.* (2008) LNA-mediated microRNA silencing in non-human primates. *Nature*, **452**, 896–899.

17. Thomas,J.R. and Hergenrother,P.J. (2008) Targeting RNA with small molecules. *Chem. Rev.*, **108**, 1171–1224.

18. Albrecht,C.H., Clausen-Schaumann,H. and Gaub,H.E. (2006) Differential analysis of biomolecular rupture forces. *J. Phys. Condens. Matter*, **18**, S581–S599.

19. Severin,P.M., Ho,D. and Gaub,H.E. (2011) A high throughput molecular force assay for protein-DNA interactions. *Lab Chip*, **11**, 856–862.

20. Albrecht,C., Blank,K., Lalic-Multhaler,M., Hirler,S., Mai,T., Gilbert,I., Schiffmann,S., Bayer,T., Clausen-Schaumann,H. and Gaub,H.E. (2003) DNA: a programmable force sensor. *Science*, **301**, 367–370.

21. Blank,K., Mai,T., Gilbert,I., Schiffmann,S., Rankl,J., Zivin,R., Tackney,C., Nicolaus,T., Spinnler,K., Oesterhelt,F. *et al.* (2003) A force-based protein biochip. *Proc. Natl Acad. Sci. USA*, **100**, 11356–11360.

22. Dose,C., Ho,D., Gaub,H.E., Dervan,P.B. and Albrecht,C.H. (2007) Recognition of ''mirror-image'' DNA by small molecules. *Angew. Chem. Int. Ed. Engl.*, **46**, 8384–8387.

23. Ho,D., Falter,K., Severin,P. and Gaub,H.E. (2009) DNA as a force sensor in an aptamer-based biochip for adenosine. *Anal. Chem.*, **81**, 3159–3164.

24. Xia,Y. and Whitesides,G.M. (1998) Soft lithography. *Annu. Rev. Mater. Sci.*, **28**, 153–184.

25. Wiegand,G., Neumaier,K.R. and Sackmann,E. (1998) Microinterferometry: three-dimensional reconstruction of surface microtopography for thin-film and wetting studies by interference contrast microscopy (RICM). *Appl. Opt.*, **37**, 6892–6905.

26. Ho,D., Dose,C., Albrecht,C.H., Severin,P., Falter,K., Dervan,P.B. and Gaub,H.E. (2009) Quantitative detection of small molecule/DNA complexes employing a force-based and label-free DNA-microarray. *Biophys. J.*, **96**, 4661–4671.

27. Vicens,Q. and Westhof,E. (2001) Crystal structure of paromomycin docked into the eubacterial ribosomal decoding a site. *Structure*, **9**, 647–658.

28. Fourmy,D., Recht,M.I., Blanchard,S.C. and Puglisi,J.D. (1996) Structure of the A site of *Escherichia coli* 16 S Ribosomal RNA complexed with an aminoglycoside antibiotic. *Science*, **274**, 1367–1371.

29. Anderson,P.C. and Mecozzi,S. (2007) Minimum sequence requirements for the binding of paromomycin to the rRNA decoding site A. *Biopolymers*, **86**, 95–111.

30. Recht,M.I., Fourmy,D., Blanchard,S.C., Dahlquist,K.D. and Puglisi,J.D. (1996) RNA Sequence determinants for aminoglycoside binding to an A-site rRNA model oligonucleotide. *J. Mol. Biol.*, **262**, 421–436.

31. Sanborn,M.E., Connolly,B.K., Gurunathan,K. and Levitus,M. (2007) Fluorescence properties and photophysics of the sulfoindocyanine Cy3 linked covalently to DNA. *J. Phys. Chem. B*, **111**, 11064–11074.

32. Levitus,M. and Ranjit,S. (2011) Cyanine dyes in biophysical research: the photophysics of polymethine fluorescent dyes in biomolecular environments. *Q. Rev. Biophys.*, **44**, 123–151.

33. Davies,B.P. and Arenz,C. (2006) A homogenous assay for micro RNA maturation. *Angew. Chem. Int. Ed. Engl.*, **45**, 5550–5552.

34. Severin,P.M. and Gaub,H.E. (2012) DNA-Protein Binding Force Chip. *Small*, **8**, 3269–3273.

SUPPLEMENTARY DATA

Characterization of fluorophores

In order to quantify the interaction of the fluorophors with the oligonucleotides to which they are conjugated, the fluorescence intensities of the middle strand and and the upper duplex are measured by means of a Fluorometer (Fluorolog3, Horiba Jobin Yvon). The oligonucleotides are diluted in 1xSSC to 0.5 µM and the duplex in a mixture of 1:1 is heated and cooled down over several hours. The excitation wavelength and emission spectra are set according to the parameters of the MFA setup. The resulting intensity curve is integrated and a quenching factor F is calculated by dividing the integrated intensity of the single strand by the integrated intensity of the duplex. Multiplying I_{Cy5}^{Start} by this factor gives the corrected normalized fluorescence.

Several repetitions yielded slightly different factors. Determining a maximum range of possible factors we could prove that the outcome of the experiment is not changed by correcting the NF with the different quenching factors. This is also visible in the Figure S1. Therefore, a medium factor was calculated and used for all analyses.
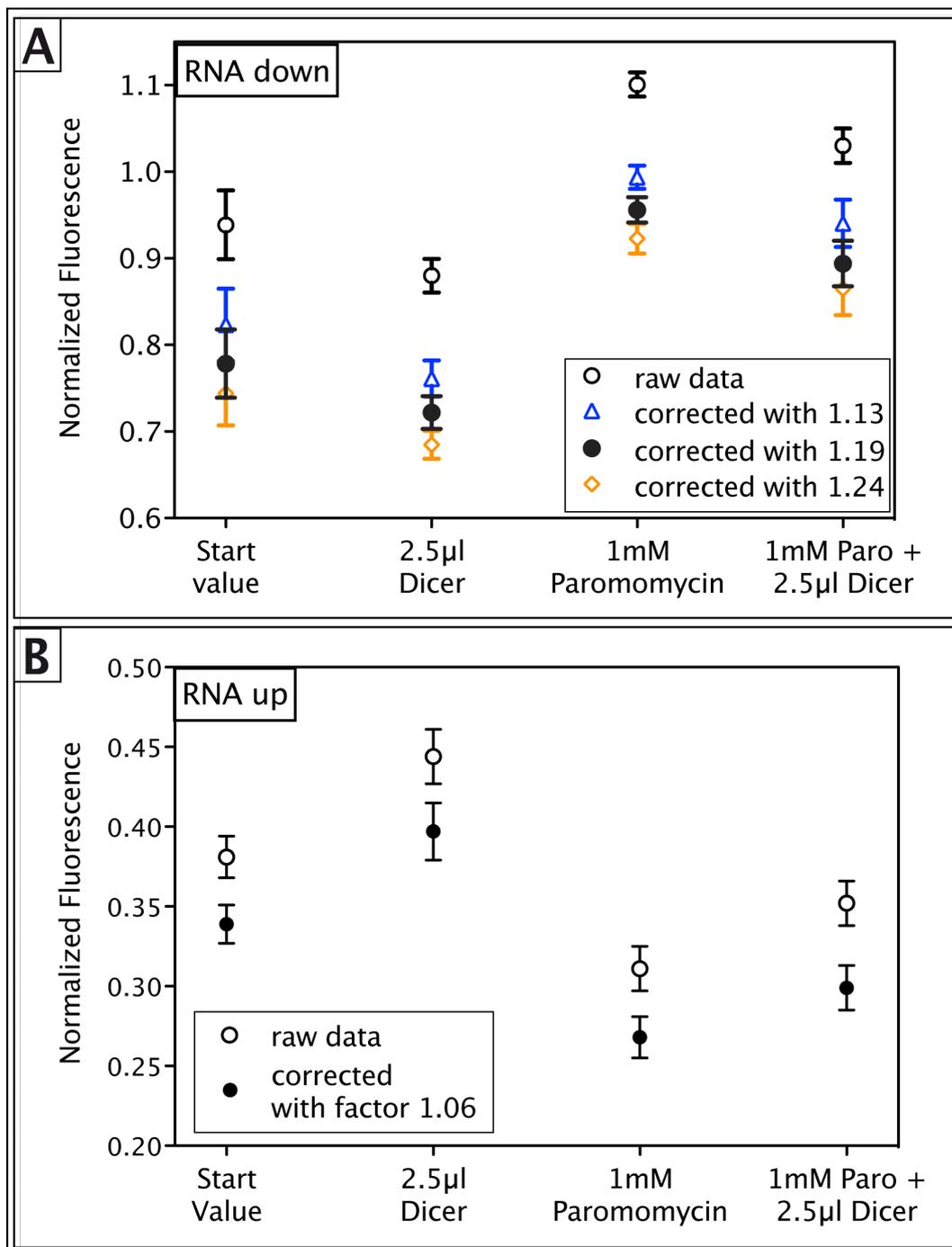
Figure S1: Proximity effects on the fluorescence intensities of Cy5.

The Cy5 with the oligonucleotide bases requires a correction of the measured fluorescence intensity in order to calculate the actual NF. A quenching factor is determined by measuring the fluorescence intensity of Cy5 conjugated to the single, middle strand as well as to the complete upper duplex by means of a fluorometer. Re-analyzing the data with a maximum range of factors does not change the outcome of the experiment. Dicer destabilizes the RNA duplex, while binding of paromomycin strengthens it. Blocking of Dicer leads to NF values close to ones of paromomycin binding. This holds true for both geometries, the RNA complex attached to the glass slide with the DNA duplex constituting the upper part (A) as well as for the inverse (B).